



Decoding the role of m⁶A Regulators in identifying and characterizing molecular subtypes of rosacea

Shuping Zhang^a, Meng Wu^a, Wenbo Xue^{b,*}

^a Department of Dermatology, Postdoctoral Station of Clinical Medicine, The Third Xiangya Hospital of Central South University, Changsha 410013, Hunan, China

^b Department of Surgery, The Third Xiangya Hospital of Central South University, Changsha 410013, Hunan, China

ARTICLE INFO

Keywords:
Rosacea
m⁶A
Subtypes
WGCNA

ABSTRACT

Rosacea is a common skin disease that predominantly affects individuals aged between 30 and 50 years. While the exact cause of the disease remains unclear, various factors have been shown to trigger or exacerbate its symptoms. N6-methyladenosine (m⁶A) modification is one of the most abundant epigenetic methylation modification in messenger RNA (mRNA) and non-coding RNA (ncRNA), plays a crucial role in RNA splicing, export, stability, and translation. In this study, we aimed to characterize m⁶A genes in rosacea, identify molecular subtypes based on m⁶A gene expression, characterize the immune features among subtypes, explore key molecules based on co-expression analysis, and identify potential targets and drugs. To achieve our objectives, we first compared the expression pattern and immune regulation of m⁶A genes between healthy and diseased groups. Then, we performed clustering to stratify disease samples into different subtypes and analyzed immune regulation and functional enrichment among the subtypes. Then, we conducted differential analysis between subtypes and applied weighted gene co-expression network analysis (WGCNA) in three subtypes. We found hub differential expression analysis (DEG) genes and their potential drug based on the WGCNA results and the drug-gene interaction database (DGIdb). Finally, *in vivo* and *in vitro* studies showed significant differences in m⁶A methyltransferase METTL3 levels in rosacea mice and control mice, as well as in the skin of rosacea patients and healthy people, while reducing METTL3 significantly inhibited the inflammatory response of human fibroblasts (HDFs) stimulated by LL37, suggesting that METTL3 may be associated with changes in overall m⁶A levels in rosacea. Taken together, our findings provide valuable insights into therapeutic targets and drug predictions for rosacea.

1. Introduction

Rosacea is a skin disease that causes redness, flushing, and inflammatory papules on the central face [1–3]. It primarily affects individuals with fair skin of Northern European descent and is estimated to impact up to 10 % of adults globally [4–8]. The physical discomfort and emotional distress caused by rosacea can be significant, as it can lead to disfigurement and mental unhealth [9,10].

The pathogeny of rosacea remains unclear, although several factors have been implicated, including genetics, immune dysregulation, neurovascular dysregulation, and environmental triggers such as sunlight, heat, and spicy foods [11–14]. Despite known

* Corresponding author.

E-mail address: xuwenbo@csu.edu.cn (W. Xue).

<https://doi.org/10.1016/j.heliyon.2023.e23310>

Received 9 May 2023; Received in revised form 23 November 2023; Accepted 30 November 2023

Available online 4 December 2023

2405-8440/© 2023 Published by Elsevier Ltd. This is an open access article under the CC BY-NC-ND license (<http://creativecommons.org/licenses/by-nc-nd/4.0/>).

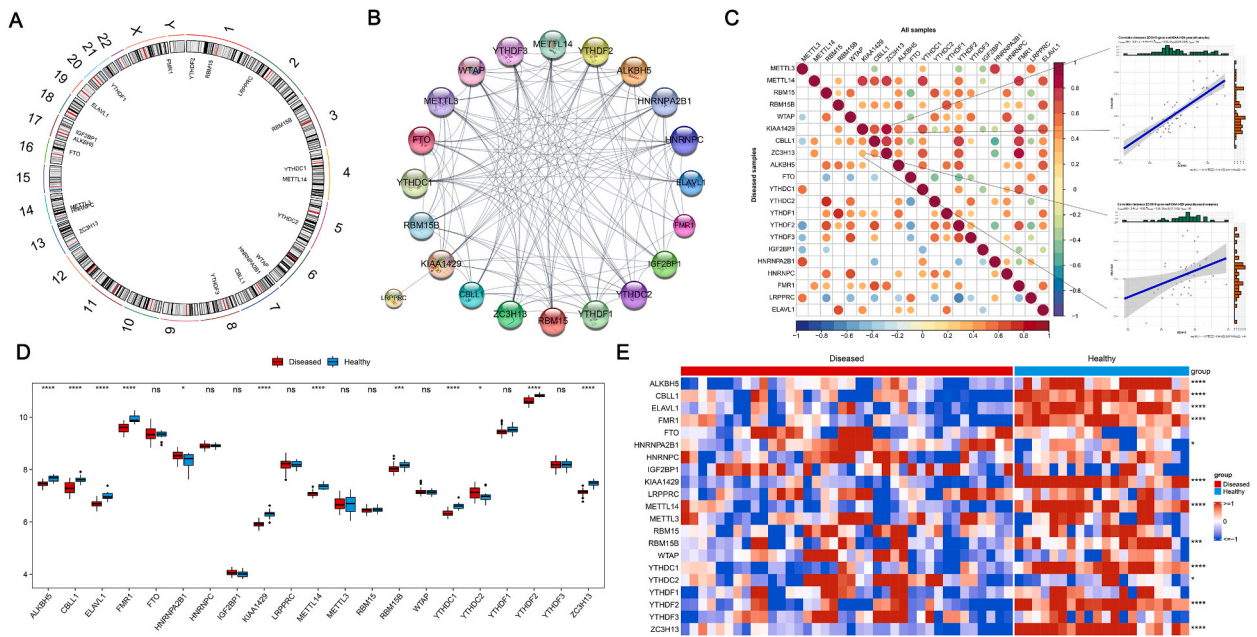


Fig. 1. The m⁶A gene landscape. (A) The chromosome location map of m⁶A genes expression. (B) The protein-protein interaction (PPI) among m⁶A genes. (C) The correlation of m⁶A gene expression levels in disease samples and all samples, with the upper right corner showing the relevance point map of m⁶A genes expression levels in all samples, and the lower left corner showing the relevance point map of m⁶A genes expression levels in disease samples. (D) The box plot of m⁶A genes expressed differentially. (E) The heat map of m⁶A genes expressed differentially.

associations, the molecular mechanisms underlying rosacea are poorly understood, and there is currently no cure for the disease. Current treatment for rosacea are limited and main purpose on managing symptoms rather than addressing underlying biological mechanisms [15–17]. Topical and oral antibiotics, topical retinoids, and other anti-inflammatory agents are commonly used to treat rosacea, but their effectiveness varies depending on the subtype and severity of the disease [18–20]. Personalized treatment options that account for the heterogeneity of the disease and address its underlying molecular mechanisms are urgently needed.

In recent years, advances in genomics and transcriptomics have allowed for the identification of molecular subtypes of various diseases, including cancer, autoimmune disorders, and neurological disorders [21–23]. These molecular subtypes have been shown to have distinct biological mechanisms and clinical features, which have important implications for diagnosis, prognosis, and treatment [24–26]. Therefore, the study aims to characterize the m⁶A genes in rosacea [27–31]. These genes play essential roles in RNA splicing, export, stability, and translation. Additionally, the study aims to recognize molecular subtypes of m⁶A genes and characterize immune features among subtypes [32–34]. Using co-expression analysis, the study seeks to identify key molecules and potential drugs for treating rosacea [35–37].

In this study, we will explore the identification and characterization of molecular subtypes of rosacea through m⁶A gene expression, with the aim of providing underlying biological mechanisms of rosacea disease and developing personalized treatment options for rosacea patients.

2. Materials and methods

2.1. Data preprocessing

To obtain data for the research, the R package GEO query was utilized to download the GSE65914 dataset of the GEO database on the GPL570 platform as the training set (<https://www.ncbi.nlm.nih.gov/geo/>) [38]. The training set involved 29 samples, consisting of 10 healthy samples and 19 disease samples. During GEO data processing, empty probes were removed, probes were transformed to gene symbols by the probe correspondence of the platform, probes meet with multiple genes were removed, and express levels were averaged for probes corresponding to the same gene symbol. The m⁶A gene was obtained from GSE15459 dataset and Table S2, which included a total of 21 genes [39].

2.2. m⁶A gene landscape

The R package R circo was utilized to depict the position of m⁶A genes on chromosomes. Using the string plugin in cytoscape software illustrated the protein-protein interaction network (PPI) of m⁶A genes. The correlation scatter plot of m⁶A genes in disease samples and all samples was drawn using the R packages stats and corplot. Additionally, differential analysis of all genes in the training

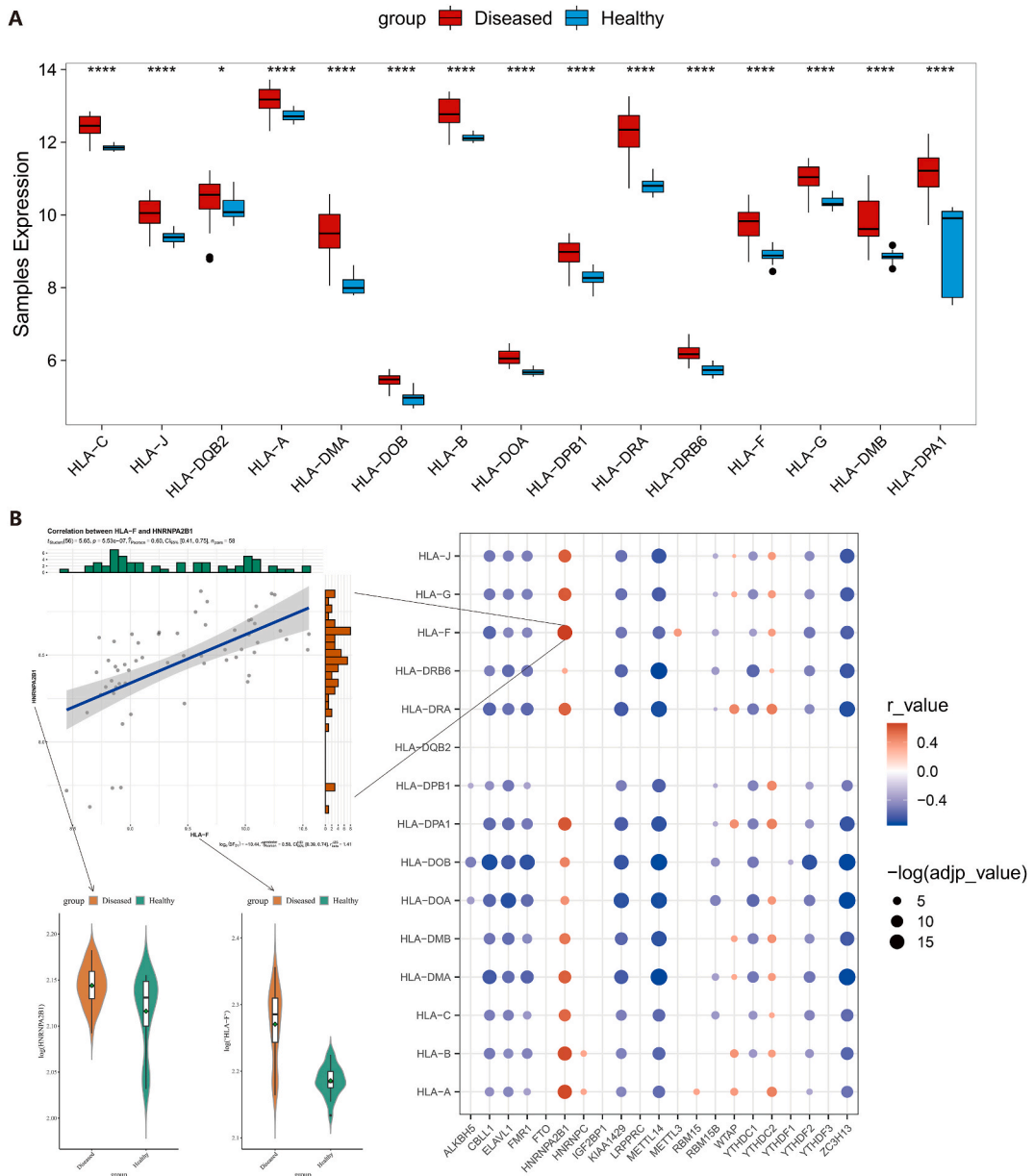


Fig. 3. (A) The analysis of HLA gene expression differences between disease and healthy groups. (B) The relevance between m⁶A gene expression levels and HLA gene expression.

in amplitude, and the sample subtype classification result was obtained from the consistency cumulative distribution function (CDF) curve. The analysis was performed on the samples using R packages stats and generated expression heatmaps and boxplots of m⁶A genes between different sample subtypes.

2.5. Functional differences between different subtypes

Pathway enrichment scores were evaluated by estimating sample scores in each pathway using KEGG gene sets and hallmark gene sets (v7.4) from the msigdb database as input data. The ssGSEA method in the R package GSVA was utilized based on the training set expression data and generated enrichment score distributions of different KEGG and hallmark pathways.

2.6. Different immune characteristics between different subtypes

Immune cell infiltration scores and immune reaction scores obtained in section 2.3. Boxplots of score differences between different

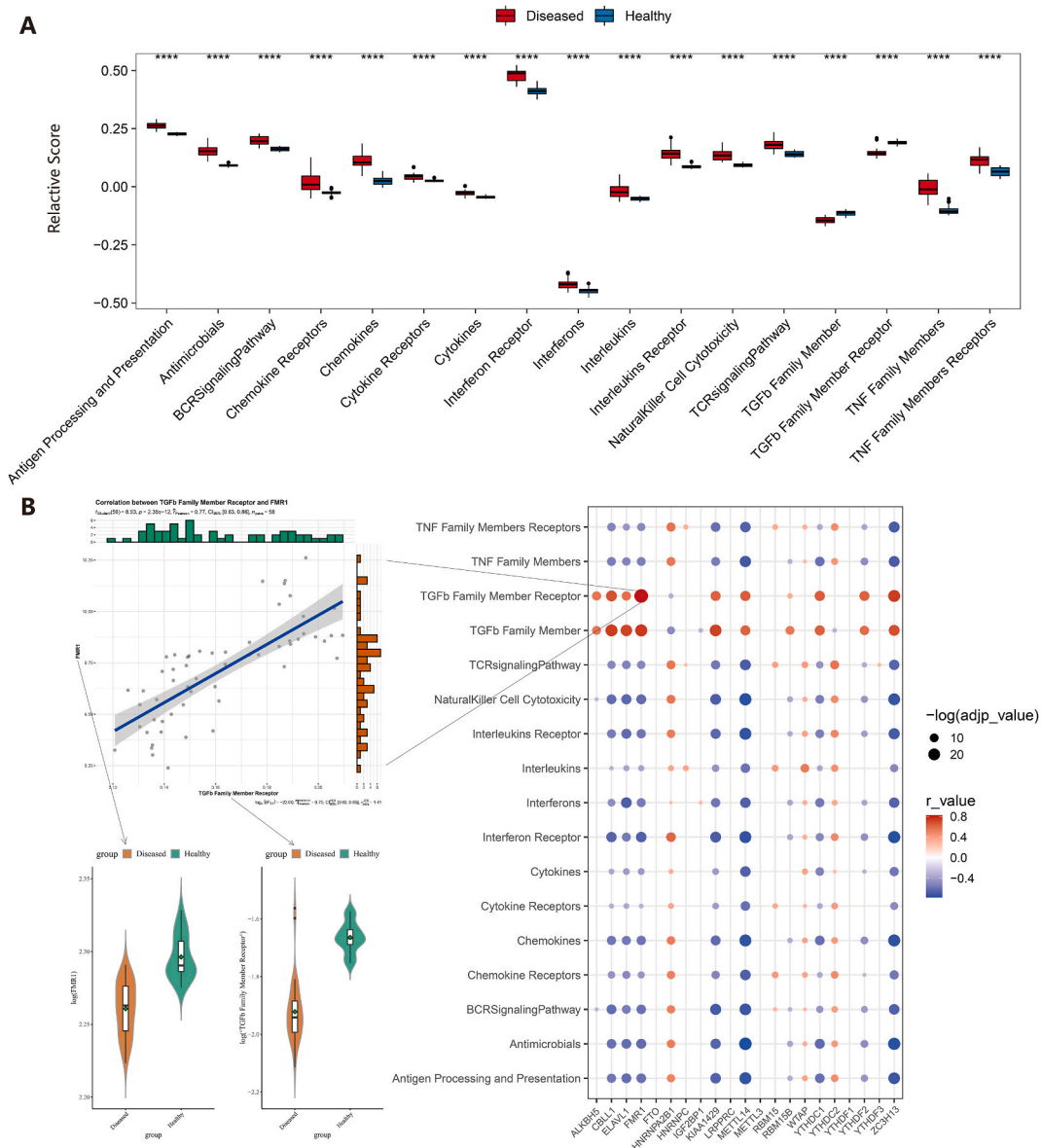


Fig. 4. (A) The analysis of immune response score differences in healthy and disease groups. (B) The relevance between m⁶A gene expression levels and immune response score.

sample subtypes and expression differences of HLA genes were generated.

2.7. Key molecules were identified based on the co-expression network approach

Using the limma package obtained differential genes between subtypes with criteria of $\text{adjust log}_2[\text{FC}] > 1$ and $p \text{ value} < 0.05$. Applying weighted gene co-expression network analysis (WGCNA) to all genes in the training set expression profile and cluster phenotype, and modules significantly related to each subtype were identified based on $\text{GS} > 0.5$ and $\text{MM} > 0.6$. Hub genes for each module and subtype were selected, and the intersection of hub genes and corresponding differential genes for each subtype was taken as the final hub DEG gene set.

2.8. Animal model

C57BL/6 mice with 6 weeks old were purchased from Slac Laboratory animal Co. Ltd (Shanghai, China) were random divided into two groups, then the mice back skin injected with LL37 peptide (320uM) for 4 times, the mice euthanized and their skins were rapidly

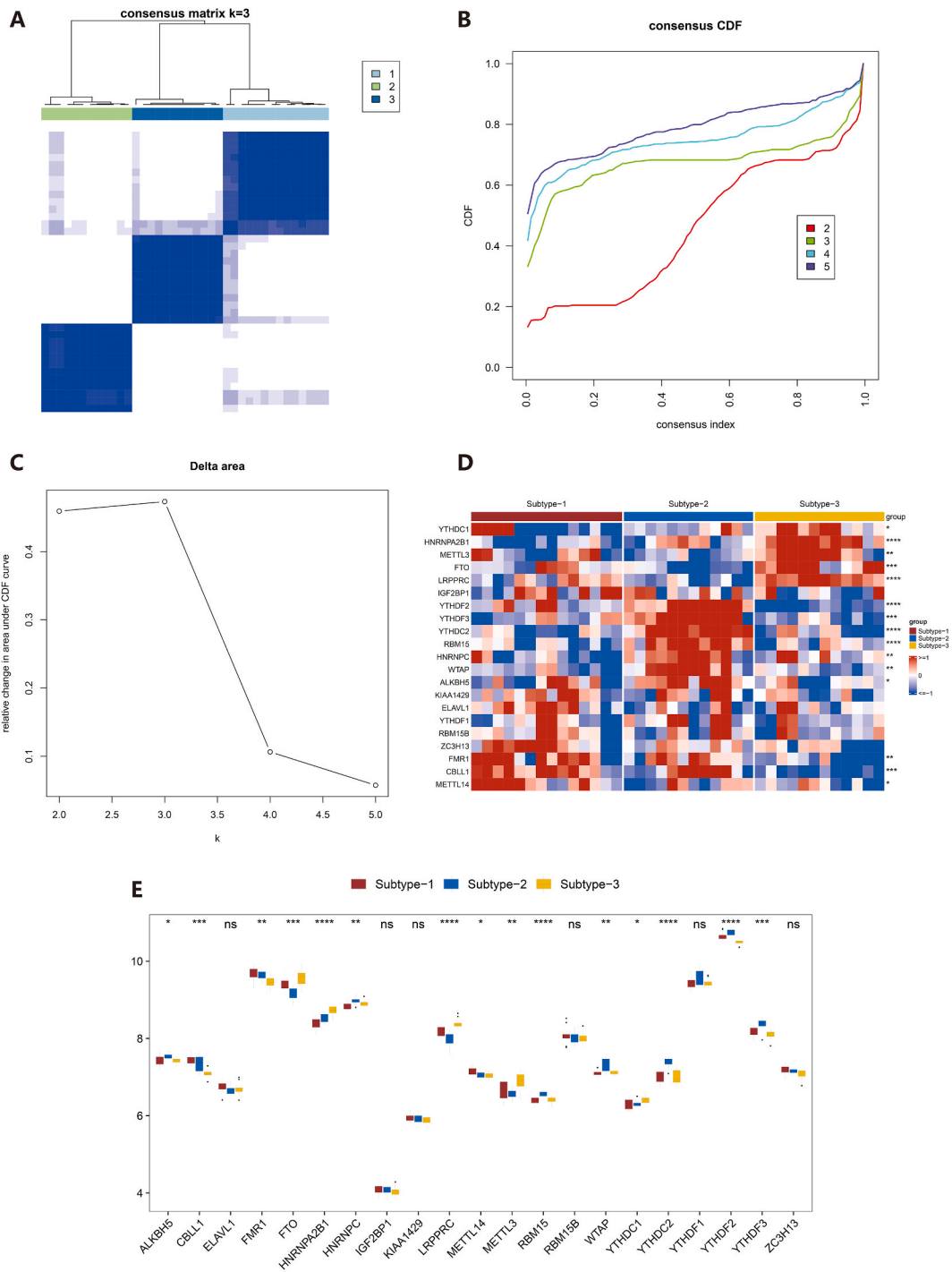


Fig. 5. The subtype classification results and related analysis. (A) The consensus clustering heatmap. (B) The cumulative distribution function (CDF) curve. (C) The area under the CDF curve relative changes. (D) The heatmap of m⁶A genes differential expression in each subtype. (E) The box plot of m⁶A genes differential expression in each subtype.

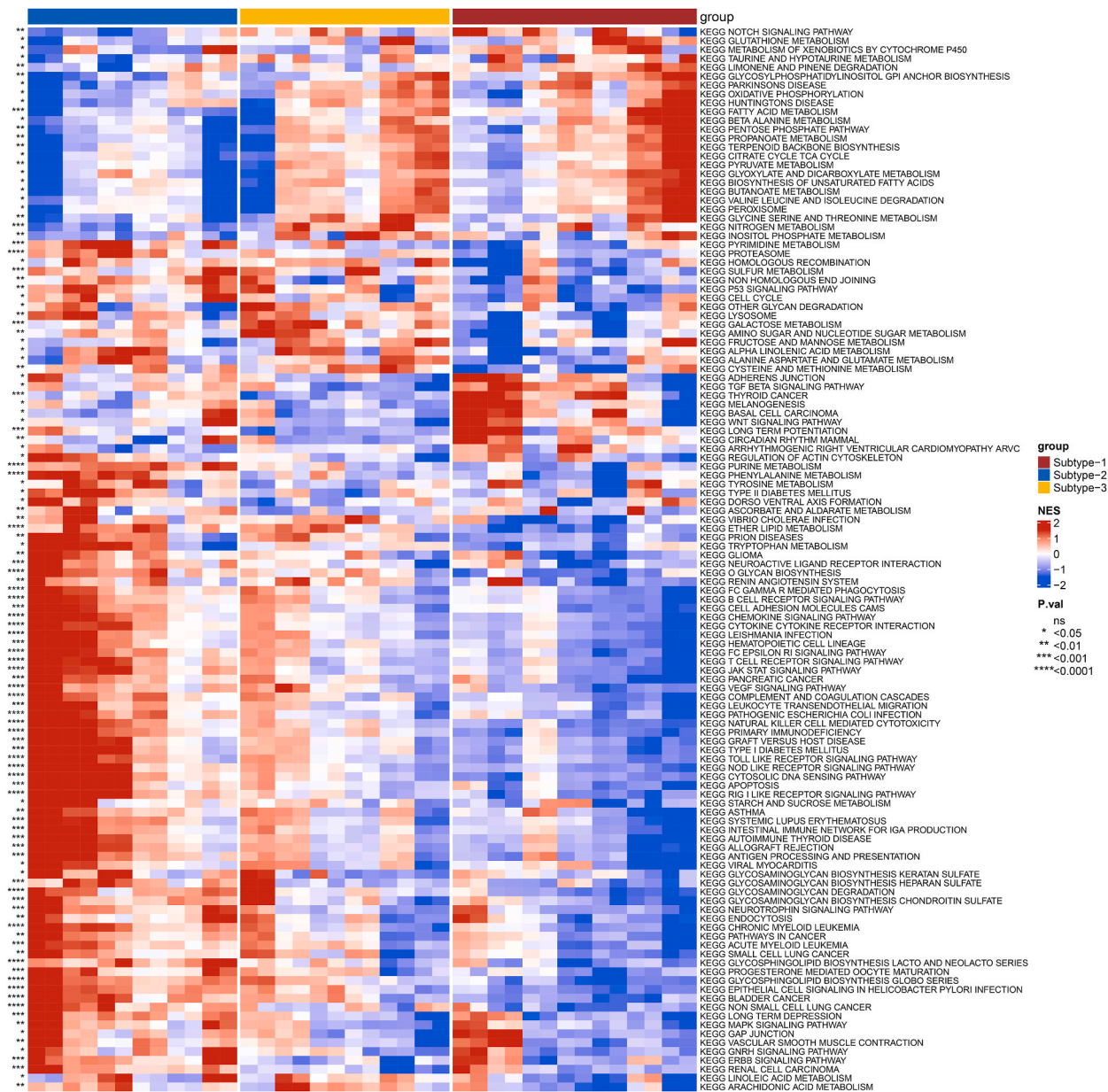


Fig. 6. The heatmap of KEGG pathway enrichment differences among subtypes.

collected. Evaluate skin inflammation of mouse model by erythema severity [42]. The animal experiments were approved by the Animal Ethics Committee of the Xiangya School of Medicine, Central South University.

2.9. Human samples

From 2020 to 2023, all skin biopsies were obtained from the central face of female healthy volunteers or patients with rosacea aged 18–60 years in the dermatology department of the Third Xiangya Hospital, Central South University. The clinical diagnosis of the rosacea subtype is made according to the classification criteria of the American Rosacea Association. The written informed consent was acquired from all participants and usage of all human tissue samples was approved by the ethical committee of The Third Xiangya Hospital of Central South University [43].

2.10. Immunohistochemistry

Fix human skin samples in formalin and embedded in paraffin, then cut into 5 μ m skin sections and use. Incubate skin sections with

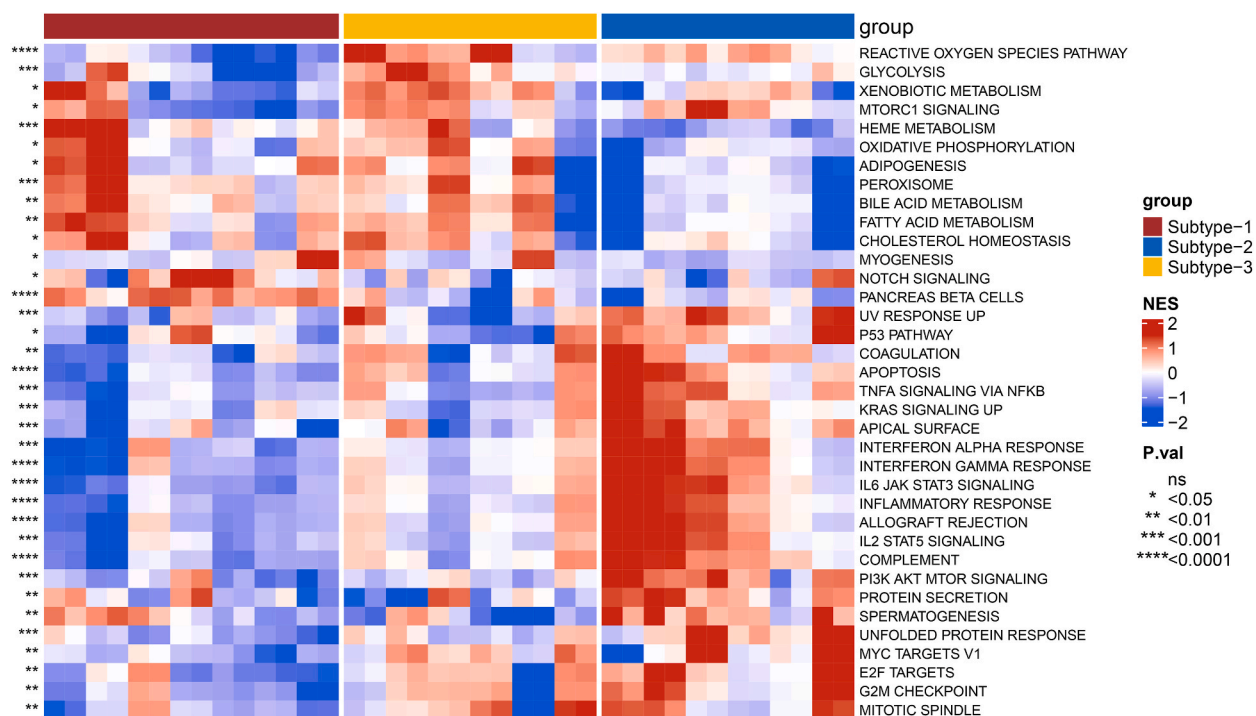


Fig. 7. The heatmap of enrichment differences of hallmark pathway among subtypes.

antibodies for METTL3 (1:200, Abcam). And take pictures from three typical areas from each skin sample and use scale of 0–4 to evaluation the intensity of staining.

2.11. Statistical analysis

When conducting differential significance analysis throughout the study, Kruskal-Wallis test was used for comparison among more than two groups. Wilcoxon test was used for pairwise comparison between two groups. In figures, "ns" equals $p > 0.05$, "*" equals $p \leq 0.05$, "**" equals $p \leq 0.01$, "***" equals $p \leq 0.001$, and "****" equals $p \leq 0.0001$.

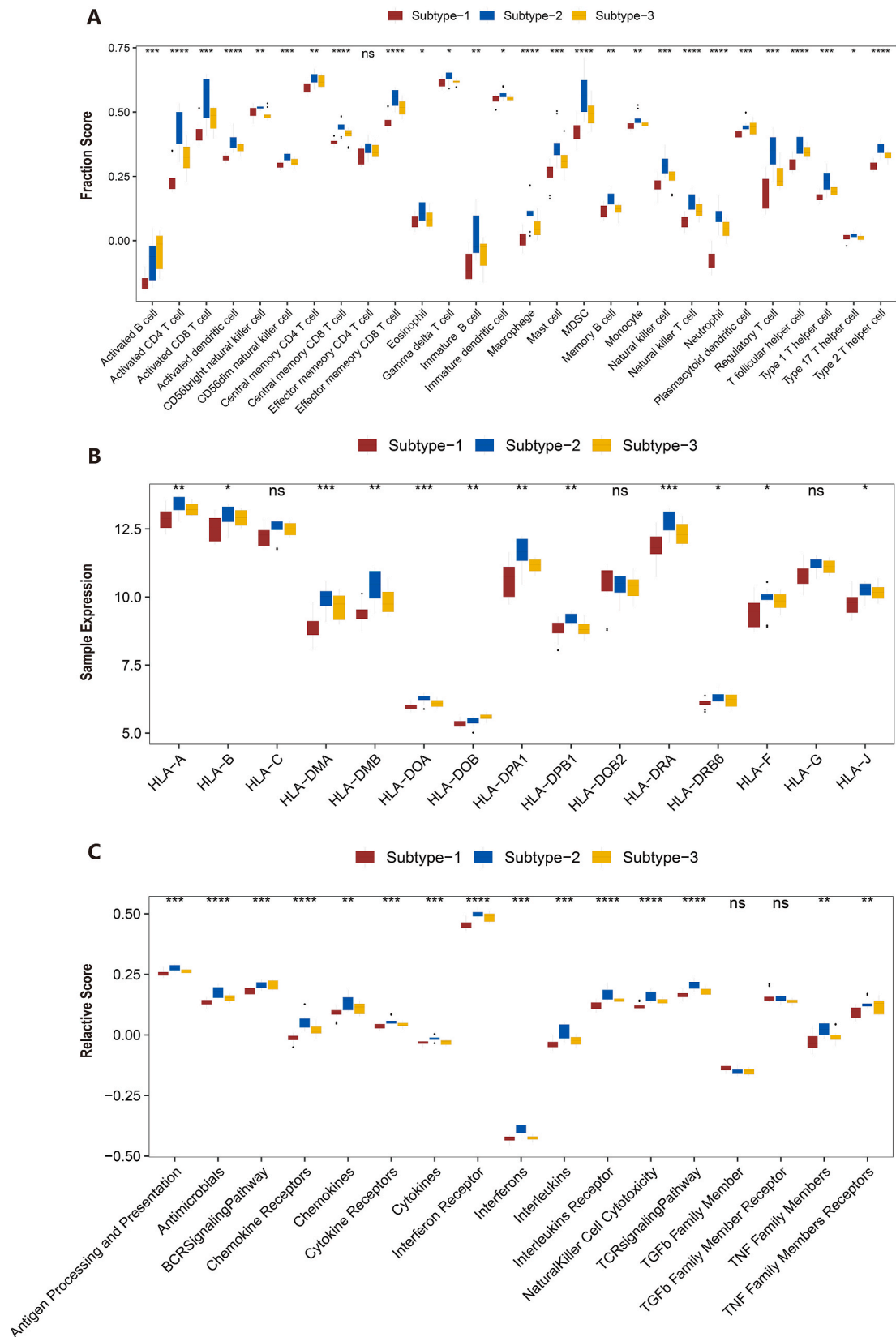
3. Results

3.1. m^6A gene landscape

We analyze the situation of m^6A genes in the training set, as shown that there was no obvious clustering of 21 m^6A genes in the chromosome (Fig. 1A). It was found that the PPI degree of all other 20 m^6A genes except for the LRPPRC gene was relatively large, indicating that these genes were closely related (Fig. 1B). It was found that the correlation of m^6A gene expression levels between all samples and disease samples was significant differences. For example, the relevance between gene ZC3H13 and KIAA1429 expression levels in all samples was 0.8, and the relevance between gene ZC3H13 and KIAA1429 expression levels in disease samples was 0.38 (Fig. 1C). It was found that the expression of 10 genes, including KIAA1429, ZC3H13, METTL14, FMR1, ELAVL1, YTHDC1, YTHDF2, CBL11, ALKBH5, and RBM15B, was downregulated significantly, while the expression of HNRNPA2B1 and YTHDC2 was upregulated significantly (Fig. 1D and E).

3.2. m^6A genes involved in disease immune regulation

It demonstrates immune infiltration scores differences between disease and healthy groups using the ssGSEA method (Fig. 2A). It was found that infiltration scores of immune cells in the disease group were higher than the healthy group. Only CD56 positive natural killer cell infiltration scores showed lower in the disease group than in the healthy group. The differences in HLA gene expression between disease and healthy groups were shown (Fig. 3A), and it was found that all 15 HLA genes in the expression profile were higher in the disease group significantly. The immune response scores between disease and healthy groups were also compared using the ssGSEA method (Fig. 4A), and it was found that the activity levels of 15 immune responses were significantly higher in the disease group (such as Antimicrobials, BCR Signaling Pathway, etc.), while TGF- β family member and its receptor were significantly more active in the healthy group. Overall, the immune activity was stronger in the disease group. The relevance between m^6A gene



(caption on next page)

Fig. 8. The different immune characteristics between three subtypes. (A) Immune infiltration scores differences between three subtypes. (B) HLA gene different expression between three subtypes. (C) Immune response scores differences between three subtypes.

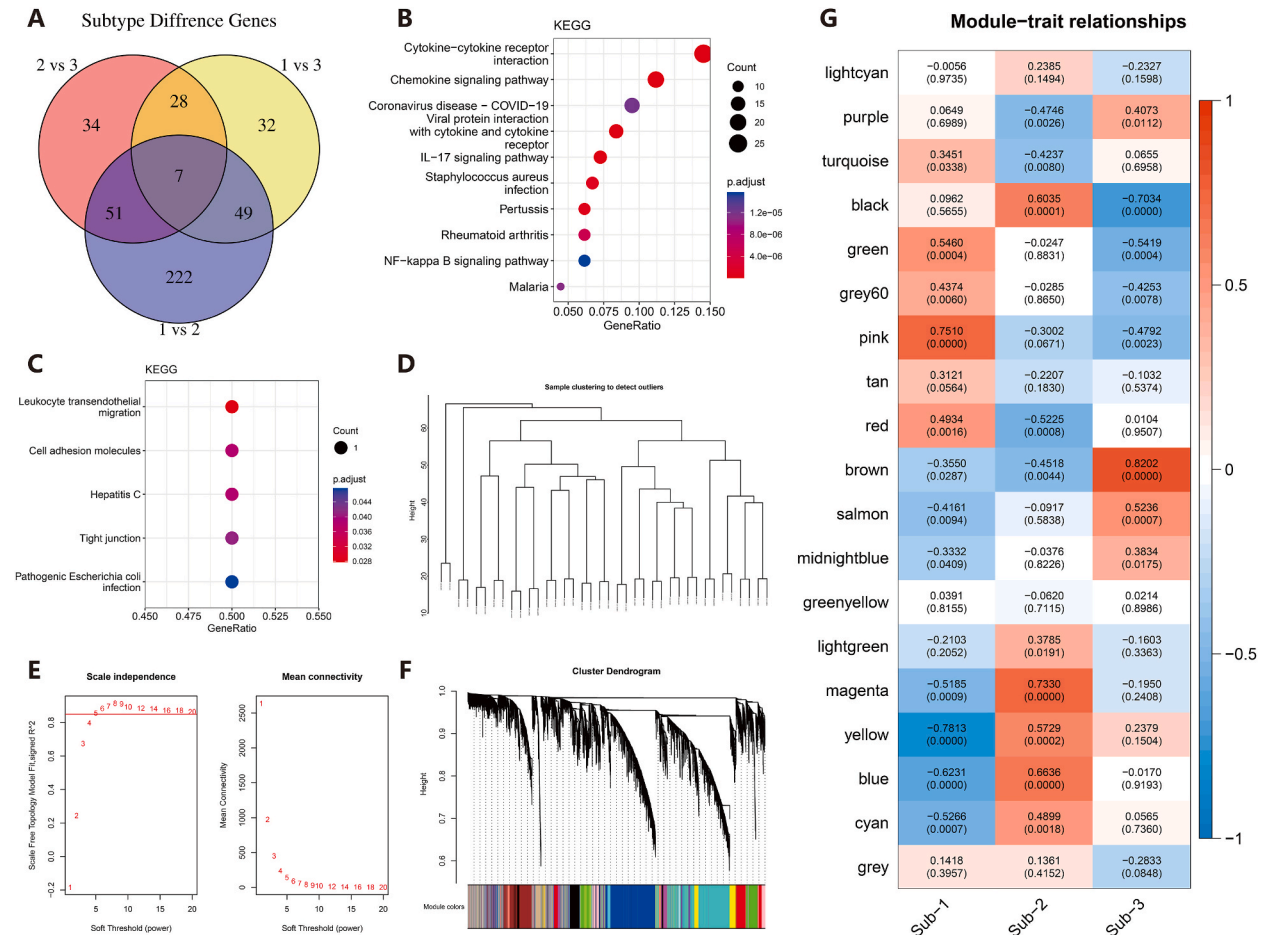


Fig. 9. The results of differential analysis and WGCNA between subtypes. (A) Venn diagram of the differential analysis results between each pair of subtypes. (B) KEGG pathway enrichment map of 423 genes obtained from the differential analysis results of the three combinations of subtypes. (C) KEGG pathway enrichment map of 7 genes obtained from the intersection of the differential analysis results for the three combinations of subtypes. (D) The training set samples in WGCNA displayed hierarchical clustering tree. (E) Corresponding scale free fit indices and Various soft thresholds, y-axis representing the scale free fit index corresponding to different soft thresholds and x-axis representing different soft thresholds. (F) WGCNA constructed the gene hierarchical clustering tree and modules (gray indicating genes that did not cluster into modules and other colors representing the modules constructed). (G) Module-phenotype correlations, with each color block representing a module, and the numbers inside the module representing the 'module-phenotype' relevance coefficient and the consequence p-value of the module in different subgroups of a phenotype. The colors are arranged from blue-white-red according to the direction of correlation values from -1 to 1 .

expression levels and immune infiltration scores (except for CD56 positive natural killer cell), HLA expression, and immune response scores were also demonstrated (Figs. 2B, 3B and 4B). It was found that CBL1, ELAVL1, FMR1, KIAA1429, METTL14, YTHDC1, and ZC3H13 were significantly negatively correlated with immune infiltration scores, HLA expression, and immune response scores (except for TGF- β family member and its receptor), while HNRNPA2B1 and YTHDC2 were significantly positively correlated with immune infiltration scores, HLA expression, and immune response scores (except for TGF- β family member and its receptor).

3.3. Using m⁶A genes categorize disease samples into biologically different subtypes

Analyze the different expression levels between subtypes by consensus clustering (Fig. 5A). The three classes with the most gradual decrease in the CDF were selected as the best clustering result (Fig. 5B and C). The differential expression of m⁶A genes in each subtype is shown in Fig. 5D and E, and it was found that 15 m⁶A genes showed differences significantly among the three subtypes.

KEGG and hallmark pathway differences between subtypes are also shown that significantly differentially enriched KEGG pathways included KEGG NOTCH SIGNALING PATHWAY and KEGG GLUTATHIONE METABOLISM, while significantly differentially enriched

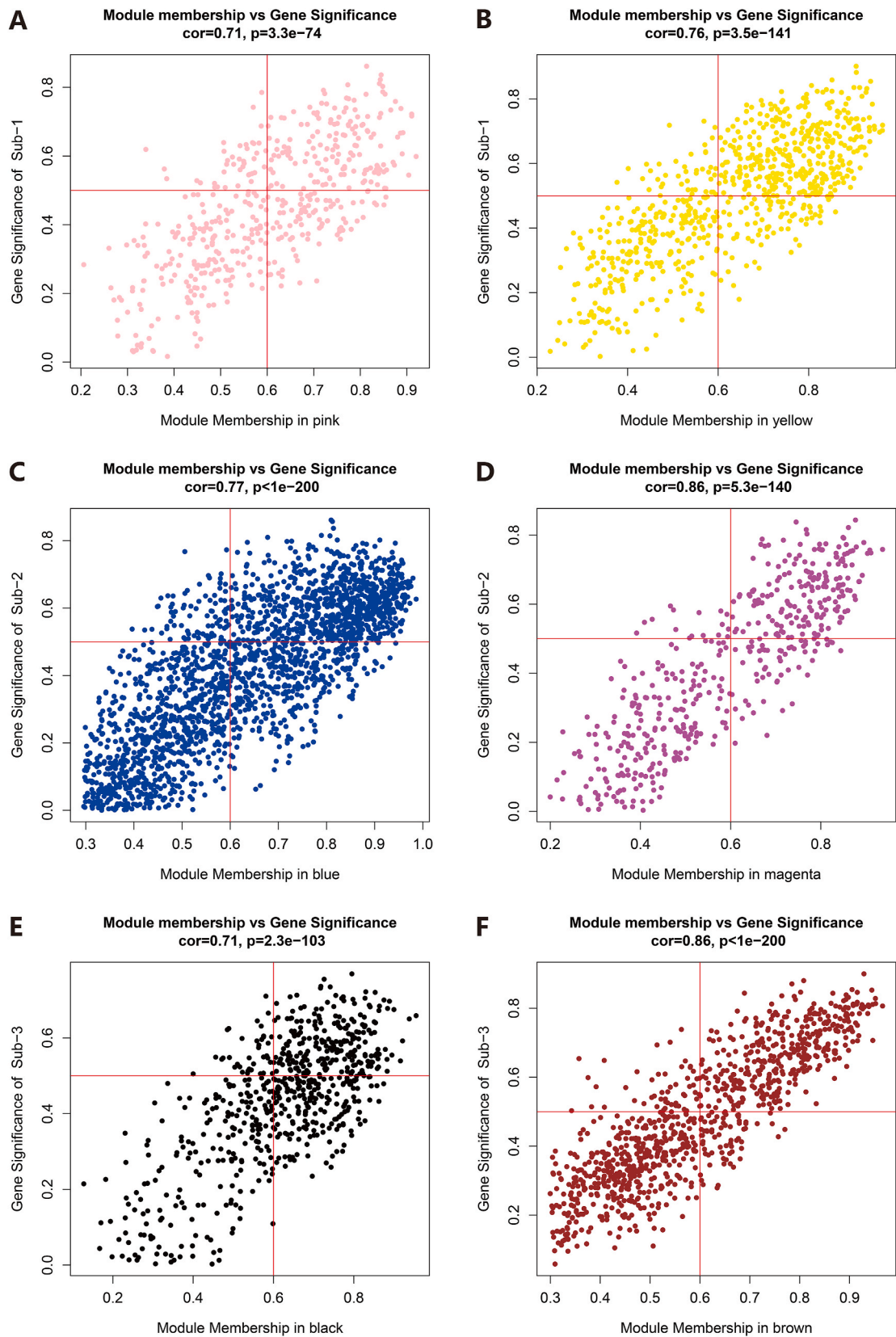


Fig. 10. MM-GS correlation scatterplots of 6 modules. (A-F) Correspond to the pink, yellow, blue, magenta, black, and brown modules, respectively.

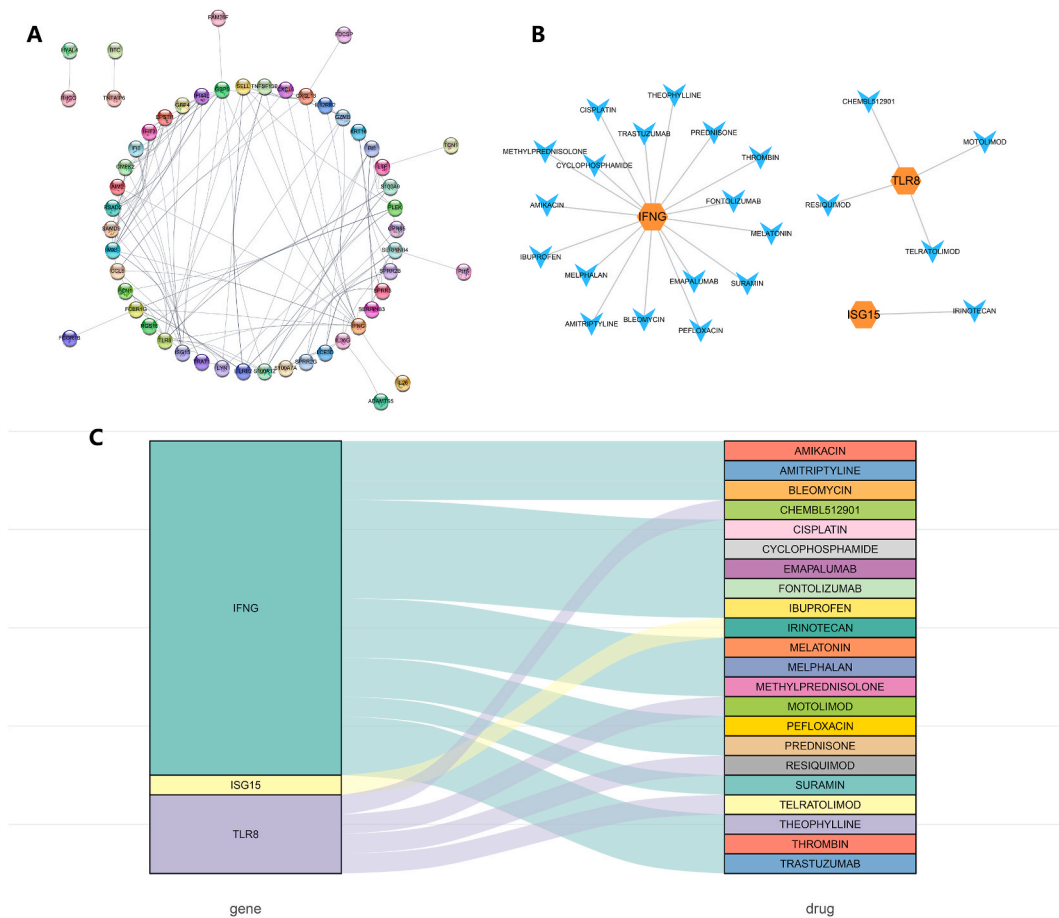


Fig. 11. The potential drug exploration of key genes. (A) PPI network of 92 hub DEG genes. (B) The top 3 genes by degree and their potential drugs. (C) Gene-drug chord diagram.

hallmark pathways included REACTIVE OXYGEN SPECIES PATHWAY and GLYCOLYSIS (Figs. 6 and 7).

3.4. Different immune characteristics among subtypes

This results show the differences in ssGSEA immune infiltration scores, HLA expression levels, and ssGSEA immune response scores between subtypes. It shows that among the 27 types of immune cells except for activated B cells, the infiltration scores were Subtype-2 is greater than Subtype-3 which is greater than Subtype-1 (Fig. 8A). And it shows that among the 12 types of HLA cells except for HLA-DOB, the expression were Subtype-2 is greater than Subtype-3 which is greater than Subtype-1 (Fig. 8B). It shows that among the 15 types of immune response scores, all immune response scores except for the BCR Signaling Pathway were Subtype-2 is greater than Subtype-3 which is greater than Subtype-1 (Fig. 8C). Therefore, it can be concluded that the sample classification is reliable, and the immune activity were Subtype-2 is greater than Subtype-3 which is greater than Subtype-1.

3.5. Recognition of key genes though Co-expression network

We performed differential analysis to identify differential genes between each subtype, and plotted a Venn diagram (Fig. 9A). Differential analysis results for the three combinations of Subtype-1, Subtype-2 and Subtype-3 were merged, resulting in 423 genes. Then we performed KEGG pathway enrichment analysis on these genes, and enriched pathways included Viral protein interaction and Cytokine-cytokine receptor interaction with cytokine and its receptor (Fig. 9B). The intersection of the differential analysis results for the three combinations resulted in seven genes and enriched pathways revealed by KEGG pathway enrichment analysis were Leukocyte *trans*-endothelial migration and Cell adhesion molecules (Fig. 9C). WGCNA was performed on all genes and cluster phenotypes, with a soft threshold of 5 used for network construction (Fig. 9D–G). Combined with the module-phenotypic correlation coefficient of Fig. 9G, pink and yellow modules are selected for Subtype-1, blue and magenta modules are selected for Subtype-2, and black and brown modules are selected for Subtype-3. Select the hub genes of the six selected modules according to the threshold $GS > 0.5$ and $MM > 0.6$ (Fig. 10A–F).

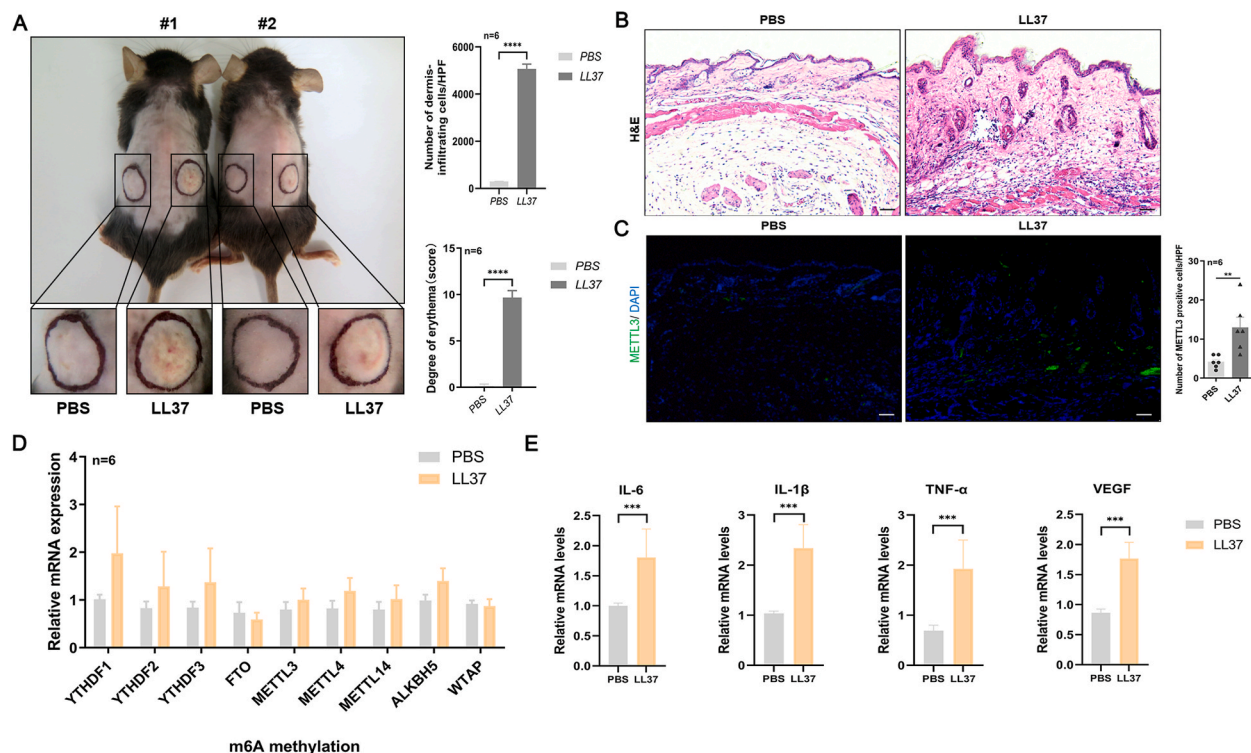


Fig. 12. The incidence of m^6A genes in rosacea mice. (A) The pictures of mice back skins injected by LL37 or control vehicle ($n = 6$). Pictures were taken on 2 days post first LL37 injection to display the representative results ($n = 6$). (B) HE staining from LL37 or control mice lesional skin. ($n = 6$). (C) Immunofluorescence showed METTL3 positive cells in control and LL37 groups. (D) The mRNA levels of m^6A genes (METTL3, METTL4, METTL14, ALKBH5, YTHDF1, YTHDF2, YTHDF3, FTO, WTAP) in mice skin lesions with LL37 or PBS control ($n = 6$). (E) IL-6, VEGF, IL-1 β , TNF- α mRNA levels in mice skin lesions with LL37 or PBS control ($n = 6$).

3.6. Potential drug mining

The module hub genes mined by each phenotype were intersected with the corresponding subtype differential genes, and 92 genes were obtained by combining the three intersection results as the final hub DEG genes. The 92 hub DEG genes were made into PPI (Fig. 11A), and the genes of degree top3 were used to mine the potential drugs of these genes (Fig. 11B and C) by using the gene-drug interaction function of DGIdb database.

3.7. Potential m^6A gene mining in rosacea mice skins

We used LL37 induced rosacea-like inflammation mouse model to further sustain above discovery, and found that the mice appeared obvious rosacea-like erythema after LL37 injection (Fig. 12A). Histological analysis showed that inflammatory cells were increased in rosacea mice compared with control mice significantly (Fig. 12B). We further mining potential m^6A gene of rosacea, like METTL3 positive cells increased in rosacea mice post LL37 injection (Fig. 12C). Remarkedly, LL37 induced rosacea mice promoted the production of methylase METTL3, METTL14 and cytokines (IL-6, VEGF, IL-1 β , TNF- α) in a much higher level than in control mice (Fig. 12D and E). Collectively, the levels of METTL3 between rosacea and control mice skin was significant differences, suggesting that METTL3 might be related to the alteration of global m^6A levels in rosacea mice skin.

3.8. Expression of m^6A genes in rosacea skins

We first detected the expression of METTL3 at mRNA level in rosacea and healthy individuals to investigate m^6A modification in rosacea. Obviously, increased METTL3 expression can be seen during rosacea skin (Fig. 13A). Then, we examined METTL3 expression in specimens from rosacea and healthy individuals. IHC showed that METTL3 levels increased in the rosacea patients skins (Fig. 13B). Human dermal fibroblasts (HDFs) participate the skin immune program via secreting pro inflammatory factors and recruiting immune cells post stimulation participate in the pathogenesis of rosacea. We thus treated the HDFs with LL37 and compared the levels of m^6A modification factors. Significantly, HDFs treated by LL37 shown higher levels of METTL3 and METTL14 compared with PBS control (Fig. 13C). To further study the increased m^6A methyltransferases METTL3 levels in rosacea, we pre-treated HDFs with METTL3 siRNA and treated cells with LL37 (Fig. 13D). RT-qPCR analysis revealed that IL-6, VEGF, IL-1 β , and TNF- α mRNA levels

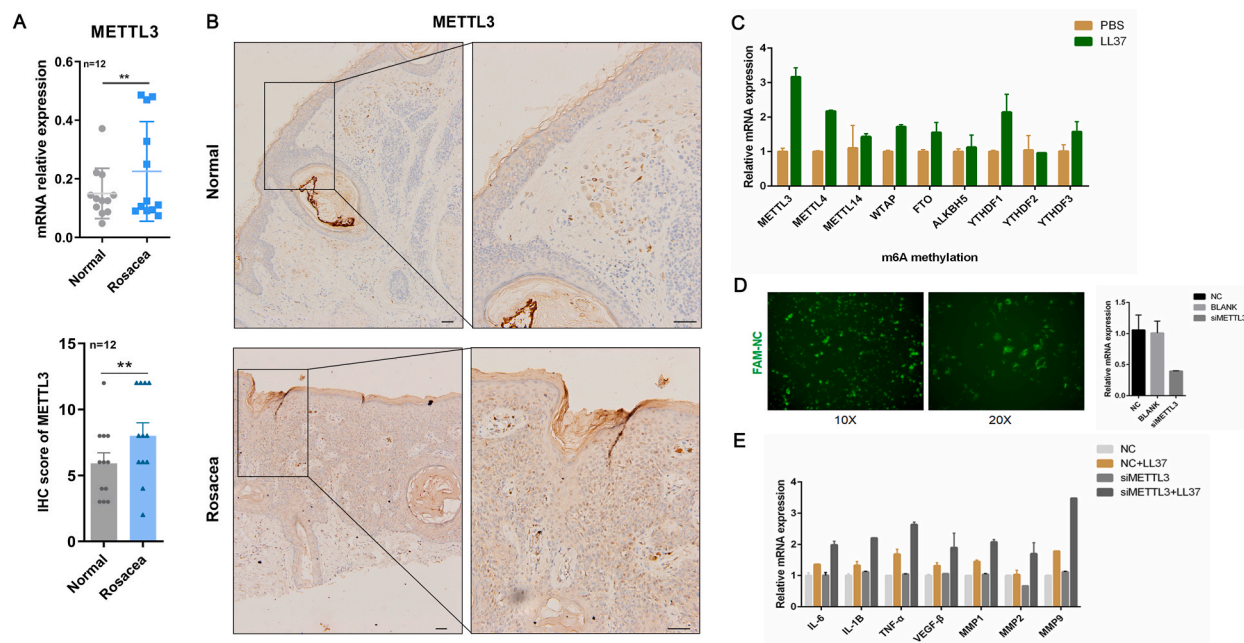


Fig. 13. The potential m⁶A genes exploration of rosacea human samples. (A) qPCR analysis of METTL3 on skin sections from normal and rosacea patients samples. (B) IHC staining of METTL3 from control or rosacea patients skins. (C) The mRNA of m⁶A levels of Human dermal fibroblasts (HDFs) treated with LL37 for 24h. (D) Immunofluorescence (IF) and qPCR analysis of METTL3 from HDFs treated with METTL3 siRNAs after LL37 treated. (E) The mRNA of cytokines and chemokines from HDFs treated with METTL3 siRNAs after LL37 treated.

were inhibited by knockdown of METTL3 (Fig. 13D and E). Consequently, reduction of METTL3 significantly suppressed inflammatory response in HDFs with LL37 stimulation. To sum up, these results demonstrated that m⁶A methyltransferases METTL3 aggravated rosacea symptoms development.

4. Discussion

The study was to investigate the m⁶A gene landscape and immune regulation differences between disease and healthy samples. A consensus clustering analysis was conducted to classify sample subtypes based on m⁶A gene expression and pathway enrichment [44]. The results showed significant differences in m⁶A genes and KEGG & hallmark pathways among subtypes. Furthermore, the study demonstrated that Subtype-2 exhibited the highest degree of immune activity, followed by Subtype-3 and then Subtype-1 [45].

The study also analyzed genes differential expression between three subtypes and identified 92 hub DEG genes related to WGCNA modules. PPI analysis was conducted on these 92 hub DEG genes, and the top 5 genes with high degree were identified. The study then explored potential drugs for these genes through the gene-drug interaction function in the DGIdb database.

Overall, this study provides valuable insights into the m⁶A gene landscape, immune regulation differences among subtypes, and potential drugs for hub DEG genes related to WGCNA modules. The molecular subtypes based on m⁶A gene expression could help reveal rosacea underlying mechanisms and lead to more personalized treatments potentially. Characterizing immune features among subtypes could provide insights into the immune response involved in rosacea development, and identifying key molecules through co-expression analysis could offer new targets for drug therapy. The study's outcomes could contribute to understanding the pathogenesis of rosacea and facilitate the development of effective treatment strategies. However, further research and validation are necessary before applying these findings clinically. These findings have significant implications for developing new therapies and treatments for diseases associated with m⁶A gene dysregulation.

Examining the impact of LL37-induced m⁶A modifications on gene expression in human rosacea skin and a rosacea mice model revealed an increase in mRNA expressions of m⁶A methylation genes. This suggests a positive correlation between m⁶A abundance and mRNA levels in LL37-treated fibroblasts. Moreover, our findings indicate that m⁶A modification of mRNAs regulates gene expression by influencing translation efficiency and stability. Notably, METTL3 exhibited significant differential modification levels in LL37-treated HDFs, leading us to speculate that this distinct methylase may contribute to the observed alterations in mRNA expression induced by LL37 and play a role in rosacea potentially.

In summary, our research indicates a substantial elevation in the overall m⁶A modification level in LL37-treated dermal fibroblasts and in rosacea skin. Utilizing genome-wide profiling of m⁶A-tagged mRNAs and subsequent bioinformatics analysis, we uncovered potential functions of transcripts with modified m⁶A in rosacea skin. These findings offer novel insights into LL37-induced rosacea and suggest potential targets for treating rosacea in human skin.

Funding sources

This work was supported from the National Natural Science Foundation of China (No. 82273508) and China Postdoctoral Science Foundation funded project (No. 2022M713537).

Ethical statement

This study was reviewed and approved by The IRB of Third Xiangya Hospital Ethics Committee, with the approval number: 2022-S171. All participants provided informed consent to participate in the study. Animal ethical approval adheres to ARRIVE guidelines and the Institutional Experimental Animal Committee of Central South University, with the approval number: XMSB-2022-0167.

Data availability statement

The data generated in this study are available upon request from the corresponding author. Data included in article/supp. Material/referenced in article.

CRediT authorship contribution statement

Shuping Zhang: Writing – review & editing, Writing – original draft, Resources, Project administration, Funding acquisition, Data curation, Conceptualization. **Meng Wu:** Writing – original draft, Methodology, Investigation, Formal analysis. **Wenbo Xue:** Writing – review & editing, Visualization, Validation, Supervision, Software, Resources, Project administration.

Declaration of competing interest

The authors declare that they have no known competing financial interests or personal relationships that could have appeared to influence the work reported in this paper.

Acknowledgements

We thank all individuals who participated in this work. We are grateful for the funding provided by National Natural Science Foundation of China and China Postdoctoral Science Foundation funded project. Special thanks to the support from post-doctoral station of medical aspects of specific environments, the Third Xiangya hospital, central south university.

Appendix A. Supplementary data

Supplementary data to this article can be found online at <https://doi.org/10.1016/j.heliyon.2023.e23310>.

References

- [1] N.N. Kulkarni, T. Takahashi, J.A. Sanford, Y. Tong, A.F. Gombart, B. Hinds, et al., Innate immune dysfunction in rosacea promotes photosensitivity and vascular adhesion molecule expression, *J. Invest. Dermatol.* 140 (3) (2020) 645–655 e646.
- [2] J. Li, B. Wang, Y. Deng, W. Shi, D. Jian, F. Liu, et al., Epidemiological features of rosacea in Changsha, China: a population-based, cross-sectional study, *J. Dermatol.* 47 (5) (2020) 497–502.
- [3] A.M. Two, W. Wu, R.L. Gallo, T.R. Hata, Rosacea: part I. Introduction, categorization, histology, pathogenesis, and risk factors, *J. Am. Acad. Dermatol.* 72 (5) (2015) 749–758, quiz 759–760.
- [4] R.L. Gallo, R.D. Granstein, S. Kang, M. Mannis, M. Steinhoff, J. Tan, et al., Standard classification and pathophysiology of rosacea: the 2017 update by the national rosacea society expert committee, *J. Am. Acad. Dermatol.* 78 (1) (2018) 148–155.
- [5] A.F. Alexis, V.D. Callender, H.E. Baldwin, S.R. Desai, M.I. Rendon, S.C. Taylor, Global epidemiology and clinical spectrum of rosacea, highlighting skin of color: review and clinical practice experience, *J. Am. Acad. Dermatol.* 80 (6) (2019) 1722–1729 e1727.
- [6] T.H. Rim, M.J. Kang, M. Choi, K.Y. Seo, S.S. Kim, Ten-year incidence and prevalence of clinically diagnosed blepharitis in South Korea: a nationwide population-based cohort study, *Clin. Exp. Ophthalmol.* 45 (5) (2017) 448–454.
- [7] Y. Sun, P.J. Tsai, C.L. Chu, W.C. Huang, Y.S. Bee, Epidemiology of benign essential blepharospasm: a nationwide population-based retrospective study in Taiwan, *PLoS One* 13 (12) (2018), e0209558.
- [8] S. Zierl, A. Guertler, J.A. Hildebrand, B.M. Clanner-Engelshofen, L.E. French, M. Reinholz, A comprehensive epidemiological study of rosacea in Germany, *Eur. J. Dermatol.* 31 (6) (2021) 744–751.
- [9] B.M. Clanner-Engelshofen, D. Bernhard, S. Dargatz, M.J. Flaig, U. Gieler, M. Kinberger, et al., S2k guideline: rosacea, *J Dtsch Dermatol Ges* 20 (8) (2022) 1147–1165.
- [10] S.P. Sinikumpu, H. Vahanikkila, J. Jokelainen, K. Tasanen, L. Huilaja, Ocular symptoms and rosacea: a population-based study, *Dermatology* 238 (5) (2022) 846–850.
- [11] R. Yang, C. Liu, W. Liu, J. Luo, S. Cheng, X. Mu, Correction to: botulinum toxin A alleviates persistent erythema and flushing in patients with erythema telangiectasia rosacea, *Dermatol. Ther.* 12 (10) (2022) 2295.
- [12] B.M. Clanner-Engelshofen, L.M. Stander, T. Steegmüller, T. Kammerer, L.H. Frommherz, P.C. Stadler, et al., First ex vivo cultivation of human Demodex mites and evaluation of different drugs on mite proliferation, *J. Eur. Acad. Dermatol. Venereol.* 36 (12) (2022) 2499–2503.

- [13] M. Chen, H. Xie, Z. Chen, S. Xu, B. Wang, Q. Peng, et al., Thalidomide ameliorates rosacea-like skin inflammation and suppresses NF-kappaB activation in keratinocytes, *Biomed. Pharmacother.* 116 (2019), 109011.
- [14] S.X. Chen, L.J. Zhang, R.L. Gallo, Dermal white adipose tissue: a newly recognized layer of skin innate defense, *J. Invest. Dermatol.* 139 (5) (2019) 1002–1009.
- [15] H. Wang, X. An, Z. Wang, Effect and safety of ALA-PDT combined with 1550 nm fractional therapy laser in treating rosacea, *Evid Based Complement Alternat Med* 2022 (2022), 3335074.
- [16] A. Grada, M.A. Ghannoum, C.G. Bunick, Sarecycline demonstrates clinical effectiveness against staphylococcal infections and inflammatory dermatoses: evidence for improving antibiotic stewardship in dermatology, *Antibiotics (Basel)* 11 (6) (2022).
- [17] M. Picardo, M. Ottaviani, Skin microbiome and skin disease: the example of rosacea, *J. Clin. Gastroenterol.* 48 (Suppl 1) (2014) S85–S86.
- [18] W. Fei, Y. Han, A. Li, K. Li, X. Ning, C. Li, et al., Summarization and comparison of dermoscopic features on different subtypes of rosacea, *Chin Med J (Engl)* 135 (12) (2022) 1444–1450.
- [19] A.L. Chien, D.J. Kim, N. Cheng, J. Shin, S.G. Leung, A.M. Nelson, et al., Biomarkers of tretinoin precursors and tretinoin efficacy in patients with moderate to severe facial photodamage: a randomized clinical trial, *JAMA Dermatol* 158 (8) (2022) 879–886.
- [20] F. He, M. Shen, Z. Zhao, Y. Liu, S. Zhang, Y. Tang, et al., Epidemiology and disease burden of androgenetic alopecia in college freshmen in China: a population-based study, *PLoS One* 17 (2) (2022), e0263912.
- [21] S. Morizane, A. Kajita, K. Mizuno, T. Takiguchi, K. Iwatsuki, Toll-like receptor signalling induces the expression of serum amyloid A in epidermal keratinocytes and dermal fibroblasts, *Clin. Exp. Dermatol.* 44 (1) (2019) 40–46.
- [22] M. Martinot, A.S. Korganow, M. Wald, J. Second, E. Birckel, A. Mahe, et al., Case report: a new gain-of-function mutation of STAT1 identified in a patient with chronic mucocutaneous candidiasis and rosacea-like demodicosis: an emerging association, *Front. Immunol.* 12 (2021), 760019.
- [23] Z. Zhao, T. Liu, Y. Liang, W. Cui, D. Li, G. Zhang, et al., N2-Polarized neutrophils reduce inflammation in rosacea by regulating vascular factors and proliferation of CD4(+) T cells, *J. Invest. Dermatol.* 142 (7) (2022) 1835–1844 e1832.
- [24] Y.R. Woo, H.J. Ju, J.M. Bae, M. Cho, S.H. Cho, H.S. Kim, Patient visits and prescribing patterns associated with rosacea in Korea: a real-world retrospective study based on electronic medical records, *J. Clin. Med.* 11 (6) (2022).
- [25] Y.R. Woo, J.H. Lim, D.H. Cho, H.J. Park, Rosacea: molecular mechanisms and management of a chronic cutaneous inflammatory condition, *Int. J. Mol. Sci.* 17 (9) (2016).
- [26] Z. Zhao, H. Zhu, Q. Li, W. Liao, K. Chen, M. Yang, et al., Skin CD4(+) Trm cells distinguish acute cutaneous lupus erythematosus from localized discoid lupus erythematosus/subacute cutaneous lupus erythematosus and other skin diseases, *J. Autoimmun.* 128 (2022), 102811.
- [27] S. Geula, S. Moshitch-Moshkovitz, D. Dominissini, A.A. Mansour, N. Kol, M. Salmon-Divon, et al., Stem cells. m6A mRNA methylation facilitates resolution of naive pluripotency toward differentiation, *Science* 347 (6225) (2015) 1002–1006.
- [28] S. Ke, E.A. Alemu, C. Mertens, E.C. Gantman, J.J. Fak, A. Mele, et al., A majority of m6A residues are in the last exons, allowing the potential for 3' UTR regulation, *Genes Dev.* 29 (19) (2015) 2037–2053.
- [29] M. Robinson, P. Shah, Y.H. Cui, Y.Y. He, The role of dynamic m(6) A RNA methylation in photobiology, *Photochem. Photobiol.* 95 (1) (2019) 95–104.
- [30] S. Zaccara, R.J. Ries, S.R. Jaffrey, Reading, writing and erasing mRNA methylation, *Nat. Rev. Mol. Cell Biol.* 20 (10) (2019) 608–624.
- [31] C. Liu, J. Cao, H. Zhang, J. Yin, Evolutionary history of RNA modifications at N6-adenosine originating from the R-M system in eukaryotes and prokaryotes, *Biology* 11 (2) (2022).
- [32] S. Ke, A. Pandya-Jones, Y. Saito, J.J. Fak, C.B. Vagbo, S. Geula, et al., m(6)A mRNA modifications are deposited in nascent pre-mRNA and are not required for splicing but do specify cytoplasmic turnover, *Genes Dev.* 31 (10) (2017) 990–1006.
- [33] J. Wang, S. Yan, H. Lu, S. Wang, D. Xu, METTL3 attenuates LPS-induced inflammatory response in macrophages via NF-kappaB signaling pathway, *Mediators Inflamm* 2019 (2019), 3120391.
- [34] L. Xiao, Q. Zhao, B. Hu, J. Wang, C. Liu, H. Xu, METTL3 promotes IL-1beta-induced degeneration of endplate chondrocytes by driving m6A-dependent maturation of miR-126-5p, *J. Cell Mol. Med.* 24 (23) (2020) 14013–14025.
- [35] X. Wang, Z. Lu, A. Gomez, G.C. Hon, Y. Yue, D. Han, et al., N6-methyladenosine-dependent regulation of messenger RNA stability, *Nature* 505 (7481) (2014) 117–120.
- [36] K. Shao, J. Hooper, H. Feng, Racial and ethnic health disparities in dermatology in the United States. Part 2: disease-specific epidemiology, characteristics, management, and outcomes, *J. Am. Acad. Dermatol.* 87 (4) (2022) 733–744.
- [37] A. Gurtler, S. Laurenz, The impact of clinical nutrition on inflammatory skin diseases, *J Dtsch Dermatol Ges* 20 (2) (2022) 185–202.
- [38] Y. Wang, B. Wang, Y. Huang, Y. Li, S. Yan, H. Xie, et al., Multi-transcriptomic analysis and experimental validation implicate a central role of STAT3 in skin barrier dysfunction induced aggravation of rosacea, *J. Inflamm. Res.* 15 (2022) 2141–2156.
- [39] B. Zhang, Q. Wu, B. Li, D. Wang, L. Wang, Y.L. Zhou, m(6)A regulator-mediated methylation modification patterns and tumor microenvironment infiltration characterization in gastric cancer, *Mol. Cancer* 19 (1) (2020) 53.
- [40] P. Charoentong, F. Finotello, M. Angelova, C. Mayer, M. Efremova, D. Rieder, et al., Pan-cancer immunogenomic analyses reveal genotype-immunophenotype relationships and predictors of response to checkpoint blockade, *Cell Rep.* 18 (1) (2017) 248–262.
- [41] X. Zhang, S. Zhang, X. Yan, Y. Shan, L. Liu, J. Zhou, et al., m6A regulator-mediated RNA methylation modification patterns are involved in immune microenvironment regulation of periodontitis, *J. Cell Mol. Med.* 25 (7) (2021) 3634–3645.
- [42] K. Yamasaki, A. Di Nardo, A. Bardan, M. Murakami, T. Ohtake, A. Coda, et al., Increased serine protease activity and cathelicidin promotes skin inflammation in rosacea, *Nat Med* 13 (8) (2007) 975–980.
- [43] G. Li, X. Tang, S. Zhang, Z. Deng, B. Wang, W. Shi, et al., Aging-conferred SIRT7 decline inhibits rosacea-like skin inflammation by modulating toll-like receptor 2–NF-kappaB signaling, *J. Invest. Dermatol.* 142 (10) (2022) 2580–2590 e2586.
- [44] M. Huang, S. Xu, L. Liu, M. Zhang, J. Guo, Y. Yuan, et al., m6A methylation regulates osteoblastic differentiation and bone remodeling, *Front. Cell Dev. Biol.* 9 (2021), 783322.
- [45] Y. Tong, W. Luo, Y. Gao, L. Liu, Q. Tang, Q. Wa, A randomized, controlled, split-face study of botulinum toxin and broadband light for the treatment of erythematotelangiectatic rosacea, *Dermatol. Ther.* 35 (5) (2022), e15395.